# Chapter 6

# $BF_3$ Adsorption on $Cr_2O_3(10\bar{1}2)$: Probing Surface Oxygen Anions and Lewis Basicity

## 6.1 Introduction

The study of single crystal and oriented thin film oxide surfaces has led to a number of demonstrations of structure sensitivity in oxide surface chemistry. Although these model oxide systems often allow one to control composition, stoichiometry, and cation oxidation state, they also provide an opportunity to expose surface cations and anions in well-defined local coordination geometries. These individual atomic sites are typically described in terms of their coordination numbers or alternately their degree of coordinative unsaturation. Although such descriptions have utility, they often fail to convey a sense of the inherently different chemical nature of the individual atomic sites. This is especially true when one considers surface oxygen anions of varying coordination. To date, there has been no convenient experimental method to probe the chemical nature of surface oxide species in different coordinations and local geometries. This chapter demonstrates that a simple thermal desorption experiment with $BF_3$ probe molecules can provide a site-sensitive measure of the Lewis basicity of surface oxygen species of different coordination.

The adsorption of probe molecules such as ammonia, pyridine, and carbon dioxide is commonly used for acid/base characterizations of surface sites on oxides, and acid/base characterizations have been used often to explain their catalytic behavior of oxide surfaces. The nature of acidic and basic sites on oxide surfaces can be described in

Lewis and Brønsted terms. For clean metal oxide surfaces (no surface protons or hydroxyl groups), the properties are principally described in terms of Lewis acidity and basicity. On metal oxides, coordinately unsaturated metal cations are generally thought of as Lewis acid sites, while the oxygen anions are thought of as Lewis base sites [1,2]. The electron-deficient metal cations exhibit acidic, electron-acceptor character, while the electron-rich oxygen anions exhibit basic, electron-donor character [2].

Boron halides have been investigated as alternative probe molecules for Lewis basicity because the $2p^1$ electronic structure of boron gives a potent Lewis acid when combined with a halogen [3]. The boron atom of $BF_3$ has one empty $p_z$-orbital, which is perpendicular to the plane of the molecule and has a tendency to accept an electron pair [4]. Many organic compounds such as alcohols, aldehydes, and ketones complex with $BF_3$ via charge donation from the oxygen atom to the boron atom of $BF_3$ [4]. When $BF_3$ complexes with a Lewis acid, the molecular geometry changes from planar to tetrahedral. $BF_3$ was chosen over other boron halides because it is not expected to dimerize like $BH_3$, polymerize like $BI_3$, or readily hydrolyze like $BBr_3$ and $BCl_3$ in the presence of water [3]. To our knowledge, $BF_3$ has not been used previously to probe the basicity of surface oxygen anions.

## 6.2 Experimental

For TDS experiments, all surfaces were exposed to $BF_3$ at 193 K and heated to 700 K using a linear temperature ramp of 2 K/sec. During TDS experiments, the background pressure was less than $2\times10^{-10}$ Torr between doses. Gas exposures reported in this study have not been corrected for ion gauge sensitivities.

XPS spectra were collected at 125 K from $Cr_2O_3$ $(10\bar{1}2)$ surfaces. Uniform steady-state charging occurs due to the insulating nature of $Cr_2O_3$ [5]. To reference the binding energy scale, short XPS runs were made at a sample temperature of 900 K where the conductivity of the material is sufficient to prevent charging. The Cr $2p_{3/2}$ binding energies at 900 K occur at 576.9 ± 0.2 eV for a nearly-stoichiometric surface. This value is within the range typically attributed to $Cr^{3+}$ in $Cr_2O_3$ [6-8]. The binding energy scale of all XPS spectra has been shifted to align the Cr $2p_{3/2}$ peak to 576.9 eV to compensate for the steady-state charging. XPS experiments were run at pass energies of 60 eV for the O 1s and F 1s regions and 200 eV for the B 1s region. Using Ag $3d_{5/2}$ for calibration, a FWHM of 1.06 eV and 2.1 eV is resolved for pass energies of 60 eV and 200 eV, respectively. A pass energy of 200 eV was used to achieve better signal-to-noise for the boron 1s feature since boron 1s has a small x-ray absorption cross section [9]. All XPS ratios have been determined by integrating areas under peaks using a linear background and applying Leybold atomic sensitivity factors.

## 6.3 Results

### 6.3.1 *Thermal Desorption Spectroscopy*

$BF_3$ adsorption was examined by TDS for the nearly-stoichiometric and oxygen-terminated surfaces. In simple Lewis acid/base terms, one might expect different basicities for the stoichiometric and oxygen-terminated surfaces because of the different forms of oxygen exposed at the surface. In Figure 6.1, TDS desorption traces from a 0.25 L ($1L \equiv 10^{-6}$ Torr-sec) $BF_3$ exposure are illustrated for the nearly-stoichiometric and oxygen-terminated surfaces. One $BF_3$ desorption feature with a peak temperature of 340

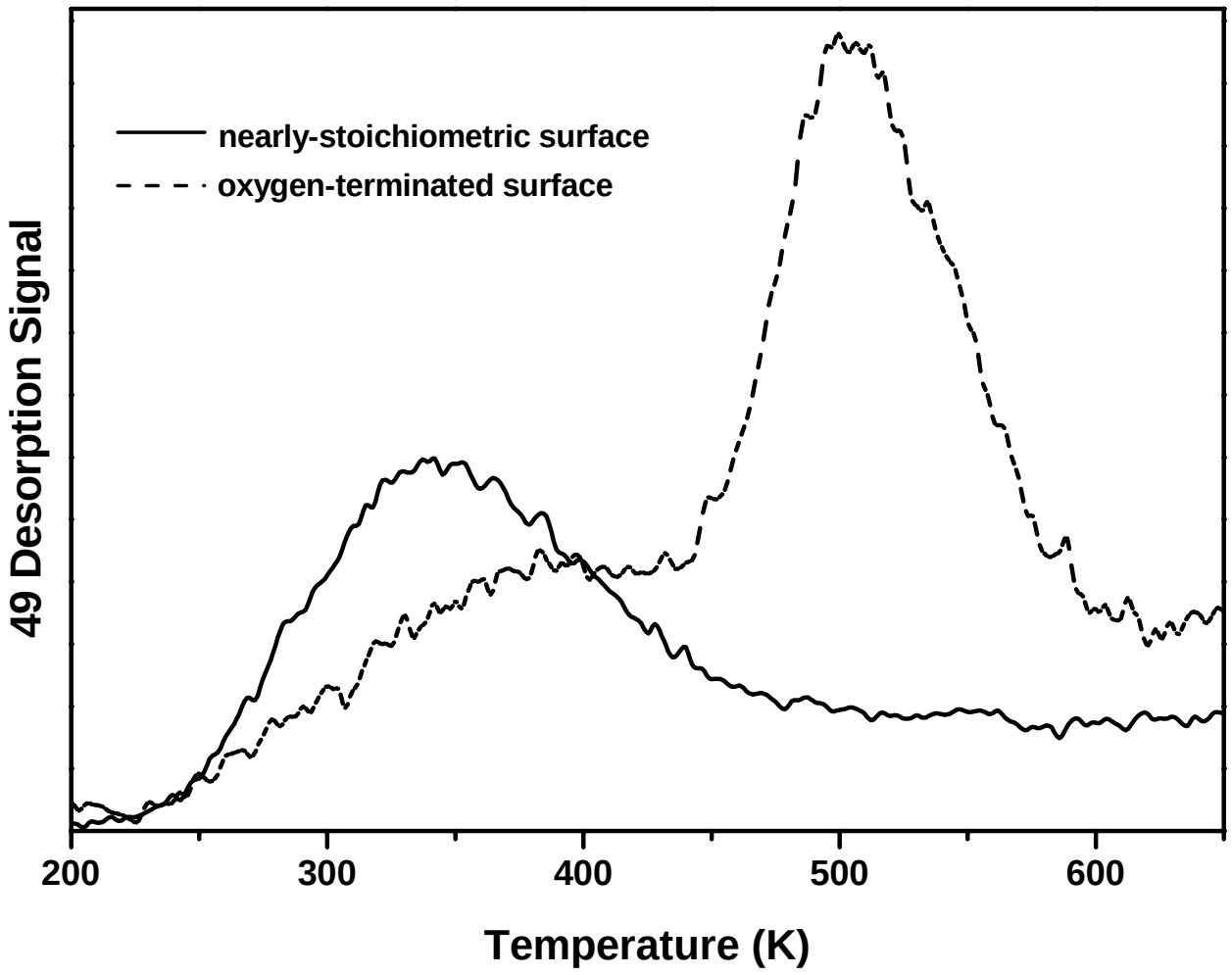


**Figure 6.1 The TDS comparison spectra shows desorption intensity versus temperature for $BF_3$ adsorbed on a nearly-stoichiometric and oxygen-terminated $Cr_2O_3$ $(10\bar{1}2)$ surface after a 0.25 L exposure.**

K is seen on the nearly-stoichiometric surface. Since the nearly-stoichiometric surface exposes predominately three-coordinate $O^{2-}$ anions, the $BF_3$ TDS feature is attributed to the adsorption of acidic $BF_3$ molecules at three-coordinate $O^{2-}$ anions. Two $BF_3$ desorption features with peak temperatures of 370 K and 500 K are seen on the oxygen-terminated surface. The $BF_3$ feature near 370 K is similar in temperature to the desorption feature seen on the nearly-stoichiometric surface. Therefore, the $BF_3$ TDS feature at 370 K on the oxygen-terminated surface is also attributed to the adsorption of acidic $BF_3$ molecules at three-coordinate $O^{2-}$ anions. Since the $BF_3$ TDS feature at 500 K appears with the introduction of terminal chromyl oxygens on the oxygen-terminated surface, the 500 K feature is attributed to the desorption of acidic $BF_3$ molecules from the terminal chromyl species (Cr=O).

The coverage dependence of the $BF_3$ desorption traces from a nearly-stoichiometric surface and an oxygen-terminated surface is illustrated in Figure 6.2. At the lowest dose investigated, 0.03 L, one $BF_3$ desorption peak is observed with a peak maximum at 370 K for the nearly-stoichiometric surface and at 550 K for the oxygen-terminated surface. With increasing $BF_3$ coverages, these features shift down in temperature to 340 K (at 0.25 L) for the nearly-stoichiometric surface and 500 K (at 0.25 L) for the oxygen-terminated surface. A second peak from the oxygen-terminated surface is seen to grow for the largest exposure of 0.25 L with a peak temperature near 370 K, near the same temperature of the $BF_3$ feature seen on the nearly-stoichiometric surface. TDS spectra are shown for only small $BF_3$ exposures, 0.03-0.25 L, due to the increasing contribution of $BF_3$ desorbed from the sample support hardware at larger exposures. A decrease in desorption temperature with coverage is often characteristic of

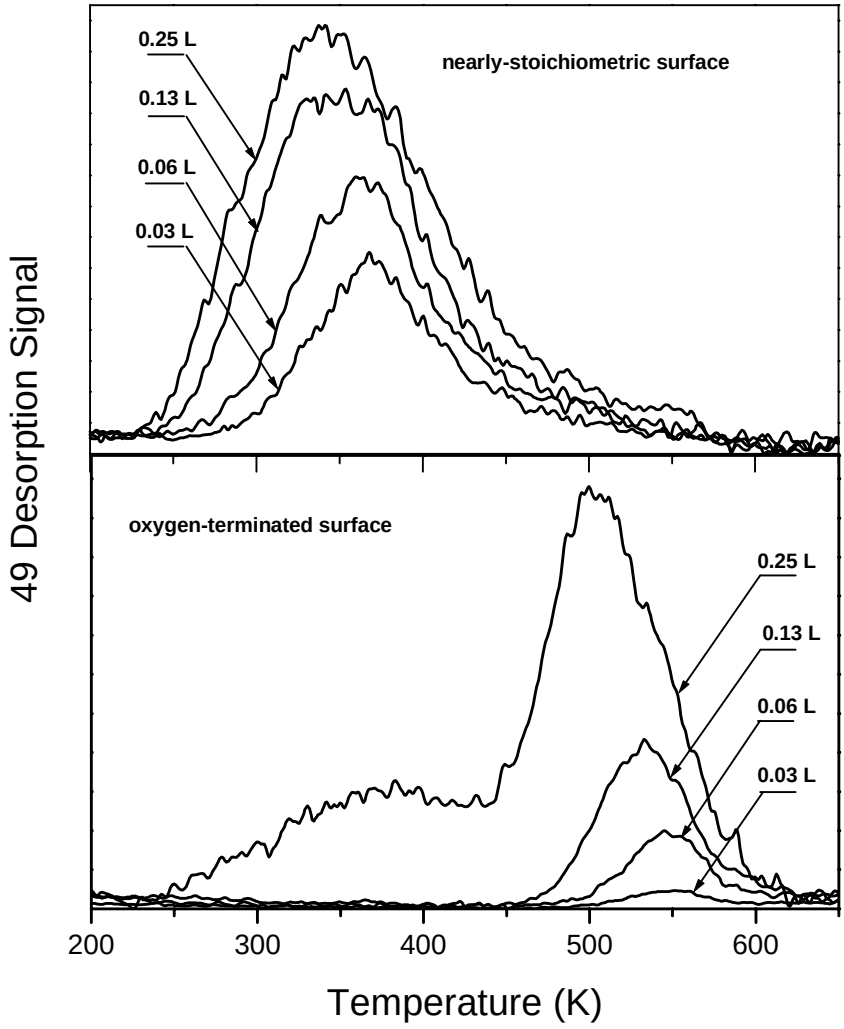


**Figure 6.2 The TDS spectra shows desorption intensity versus temperature for $BF_3$ adsorbed on a nearly-stoichiometric (top) and oxygen-terminated (bottom) $Cr_2O_3$ $(10\bar{1}2)$ surface.**

a second-order desorption process [10]. However, a second-order Redhead analysis of the TDS data shows no linearity suggestive of second-order behavior that might indicate a $BF_3$ recombination process [10]. All $BF_3$ desorption features are thought to be first-order and originate from a molecular $BF_3$ adsorbate. XPS data (below) also suggests the adsorption of molecular $BF_3$ on $Cr_2O_3$. The temperature decrease in TDS is attributed to a variation in the $1^{st}$ order activation energy for desorption with coverage. Assuming a normal pre-exponential of $10^{13}$ $s^{-1}$, the first-order activation energy for desorption is estimated from the Redhead equation to be 21.3-23.1 kcal/mol for the $BF_3$ desorption feature on the nearly-stoichiometric surface and a range of 31.8-34.9 kcal/mol for the higher temperature feature seen on the oxygen-terminated surface [10]. No attempt was made to independently determine the pre-exponential via the method of heating rate variation. The heating rate was kept intentionally low (2 K/sec) to avoid the possibility of thermal fracture of the ceramic sample.

Although the $BF_3$ desorption features are attributed to molecular surface species, $BF_3$ adsorption on $Cr_2O_3$ $(10\bar{1}2)$ is not a clean molecular adsorption/desorption process. Trace amounts of HF and $F_2$ were detected during each $BF_3$ TDS run. Hence, some $BF_3$ dissociation occurs. TDS spectra of the reaction products arising from $BF_3$ on the nearly-stoichiometric and oxygen-terminated surfaces are shown in Figure 6.3 for a 0.25 L exposure of $BF_3$. On the nearly-stoichiometric surface, HF desorbs as a broad feature with a peak temperature around 430 K, and trace amounts of $F_2$ desorb with peak temperatures of 280 K and 365 K. On the oxygen-terminated surface, HF desorbs with a peak temperature of 470 K, and trace amounts of $F_2$ desorb with a peak temperature of 310 K.

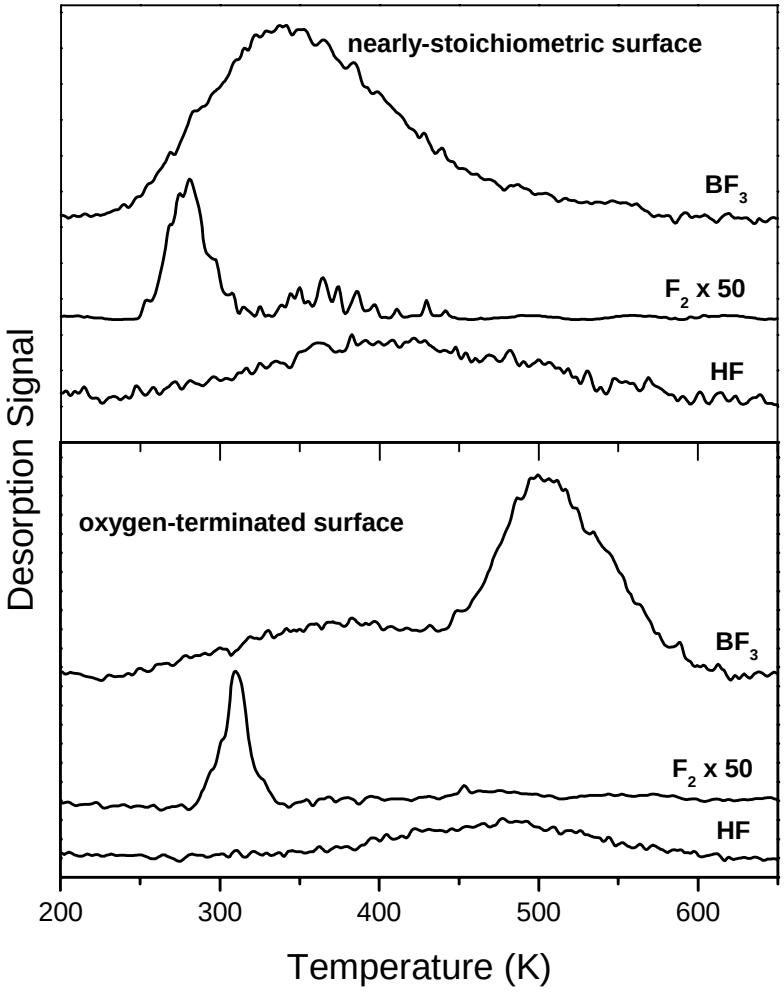


**Figure 6.3 The TDS spectra shows desorption intensity versus temperature for a 0.25 L $BF_3$ exposed nearly-stoichiometric (top) and oxygen-terminated (bottom) $Cr_2O_3$ $(10\bar{1}2)$ surface and reaction products $F_2$ and HF.**

The dissociation of $BF_3$ results in a deposition of boron and fluorine on the surface after successive TDS runs. After this build-up of boron and fluorine on the surface (a $BF_3$-modified surface), a larger amount of $BF_3$ desorption is seen from a $BF_3$-modifed surface for a given exposure of $BF_3$ compared to a clean surface that has yet to be exposed to $BF_3$. In Figure 6.4, $BF_3$ desorption traces from a 0.06 L exposure are shown for $BF_3$-modified nearly-stoichiometric and oxygen-terminated surfaces with $BF_3$ coverages similar to those shown in Figure 6.1 for a clean surface. One $BF_3$ feature at 320 K is seen on the $BF_3$-modified nearly-stoichiometric surface, and two $BF_3$ features at 340 K and 495 K are seen on the $BF_3$-modified oxygen-terminated surface. The shape and desorption temperature of these TDS features from $BF_3$-modified surfaces is nearly the same as the TDS features arising from clean surfaces. The boron and fluorine left on the surface affects $BF_3$ uptake for a given $BF_3$ exposure but not the desorption temperature for a given $BF_3$ coverage. Therefore, $BF_3$ is still able to probe surface oxygen species despite the build-up of surface boron and fluorine.

### *6.3.2 X-ray Photoelectron Spectroscopy*

X-ray photoelectron spectroscopy (XPS) was used to study the interaction between $BF_3$ with the nearly-stoichiometric and oxygen-terminated surfaces. Changes in the oxygen 1s signal upon $BF_3$ adsorption on the nearly-stoichiometric and oxygen-terminated surfaces were seen with XPS (shown in Figure 6.5). The O 1s feature on the clean nearly-stoichiometric and oxygen-terminated surface has a binding energy of 530.4 ± 0.1 eV. When the surface is exposed to 5 L of $BF_3$, an additional feature in XPS appears at a higher binding energy near 532.8 ± 0.2 eV for the nearly-stoichiometric

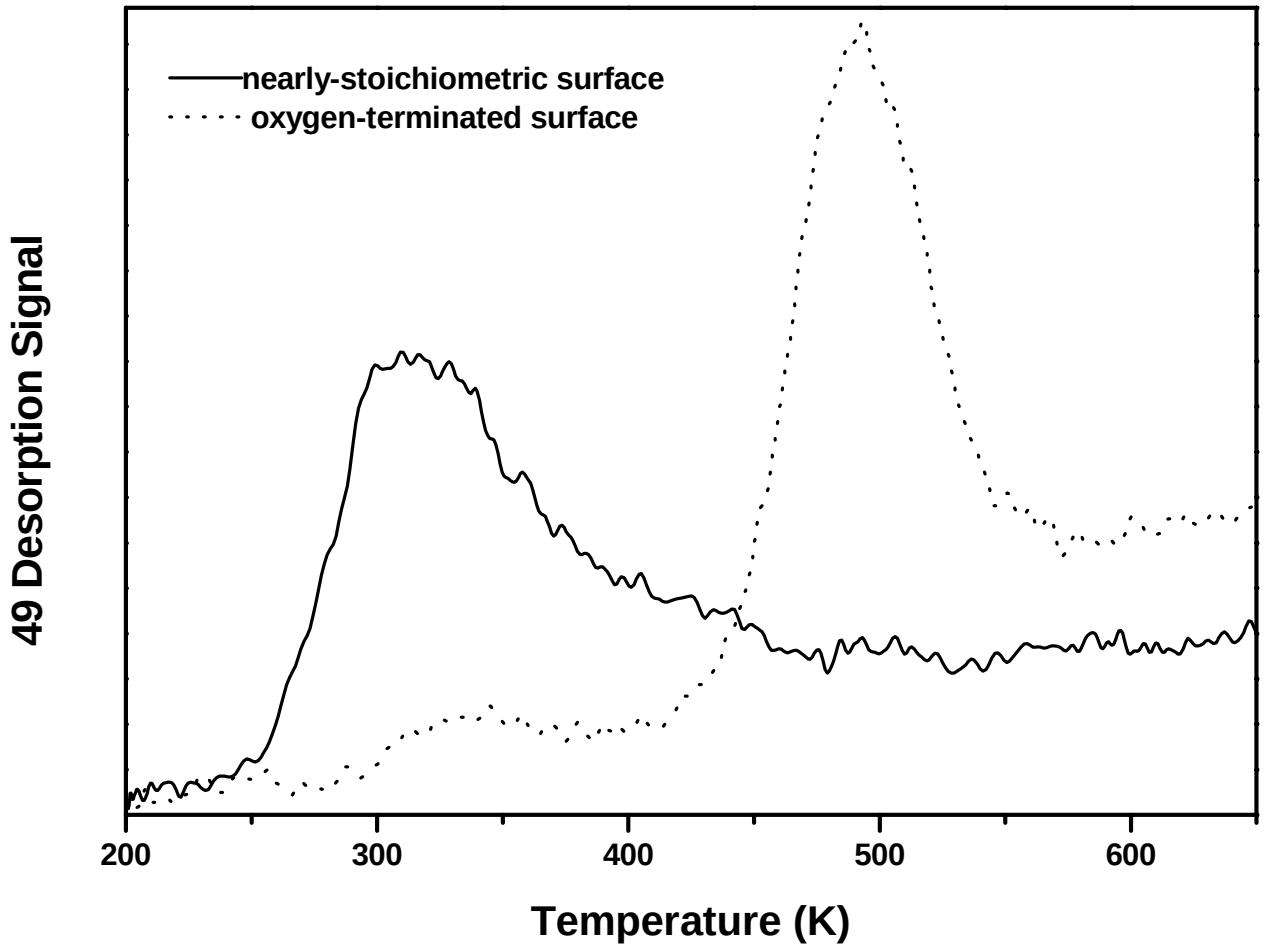


**Figure 6.4 The TDS comparison spectra shows desorption intensity versus temperature for $BF_3$ adsorbed on a $BF_3$-modified nearly-stoichiometric and boron-covered oxygen-terminated $Cr_2O_3$ $(10\bar{1}2)$ surface for a similar $BF_3$ coverage seen in Figure 6.1.**

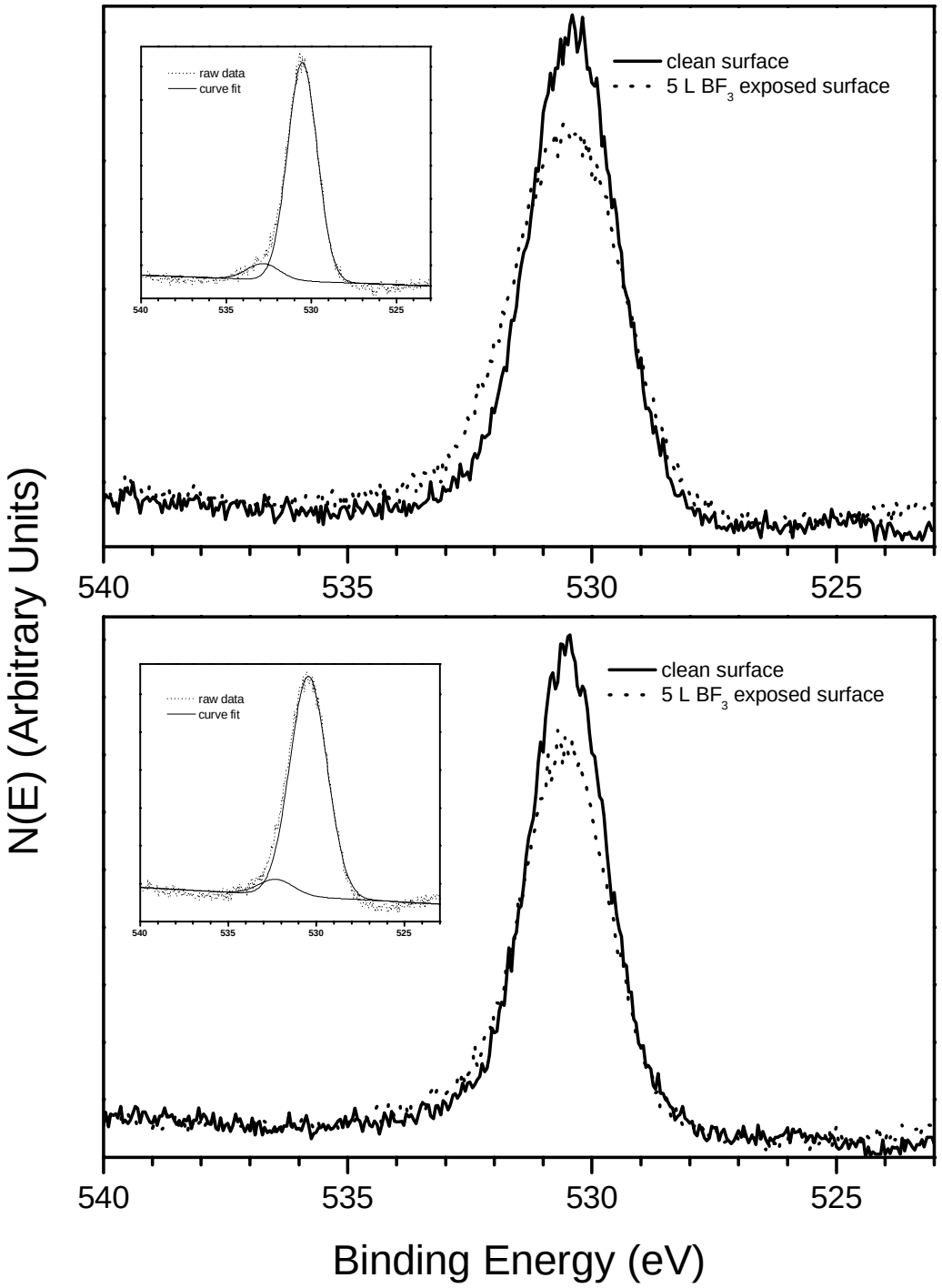


**Figure 6.5 XPS spectra shows the O 1s region of the nearly-stoichiometric $Cr_2O_3$ $(10\bar{1}2)$ surface (top) and the oxygen-terminated $Cr_2O_3$ $(10\bar{1}2)$ surface (bottom) for a clean and 5 L $BF_3$ exposed surface with two peaks resolved by peak fitting where the larger peak represents a clean surface and the smaller peak represents the $BF_3$ interaction with oxygen sites.**

surface and 532.2 ± 0.2 eV for the oxygen-terminated surface. The higher binding energy feature indicates charge transfer from surface oxygen to the adsorbed $BF_3$ and demonstrates a direct interaction of $BF_3$ with surface oxygen sites [11]. This higher binding energy feature disappears when the sample is heated to temperatures in TDS where molecular $BF_3$ is removed from the surface. Therefore, the higher binding energy oxygen 1s feature is indicative of a direct interaction between molecular $BF_3$ and surface oxygen sites to form a Lewis acid/base adduct.

The nature of the adsorbed species was investigated by XPS. The boron 1s XPS region is shown in Figure 6.6 for the nearly-stoichiometric surface (top) and the oxygen-terminated surface (bottom). On the nearly-stoichiometric surface, one broad B 1s feature appears at a binding energy of 194.1 eV with the exposure of 5 L $BF_3$. The B 1s feature shifts down to 193.1 eV upon annealing to 340 K, where all molecular $BF_3$ is removed from this surface, and the B 1s feature shifts further down to 192.0 eV after annealing to 900 K. On the oxygen-terminated surface, one broad B 1s feature appears at a binding energy of 193.8 eV with the exposure of 5 L $BF_3$. The B 1s feature shifts down to 192.8 eV upon annealing to 500 K, where all molecular $BF_3$ is removed from this surface. After annealing to 900 K, the B 1s feature shifts down to 192.3 eV. The B 1s features at 194.1 eV (nearly-stoichiometric surface) and 193.8 eV (oxygen-terminated surface) following 5 L $BF_3$ exposures are attributed to molecular $BF_3$ at surface base (oxygen) sites since the acid/base adducts $NH_3$:$BF_3$ and $C_5H_5N$:$BF_3$ have reported B 1s binding energies of 194.9 eV and 194.3 eV, respectively [8]. The 1 eV shift to lower binding energies for the B 1s feature on both surfaces after removing all molecular $BF_3$ indicates a change from molecular to dissociated $BF_3$. This lower binding energy feature

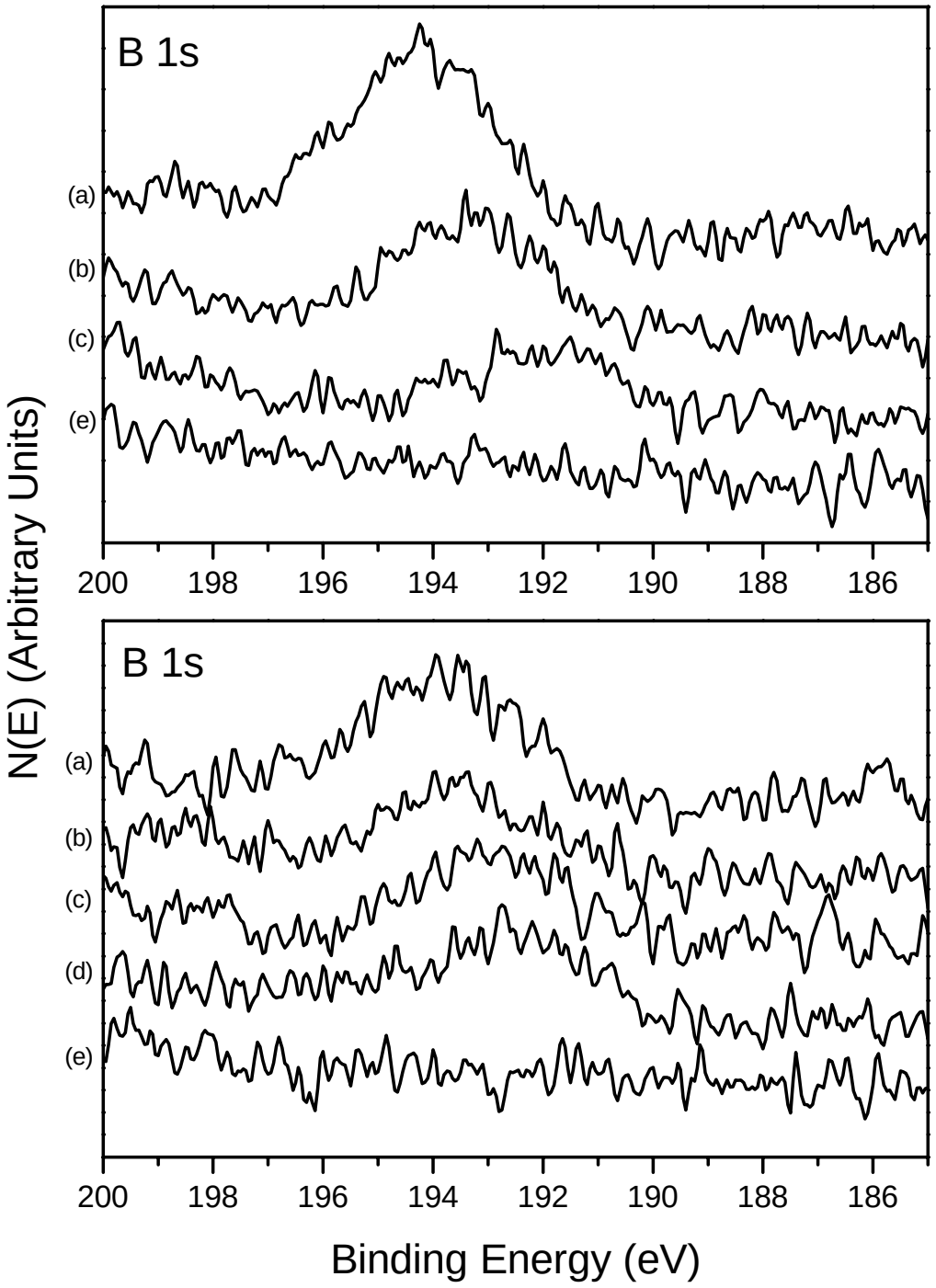


**Figure 6.6 XPS spectra shows the B 1s region of the nearly-stoichiometric $Cr_2O_3$ $(10\bar{1}2)$ surface (top) and the oxygen-terminated $Cr_2O_3$ $(10\bar{1}2)$ surface (bottom) for: (a) a 5 L $BF_3$ exposed surface, (b) a surface annealed to 340 K, (c) a surface annealed to 500 K, (d) a surface annealed to 900 K, and (e) a clean surface.**

is attributed to a combination of readsorbed molecular $BF_3$ and $BF_x$ fragments on the surface. The B 1s features on both surfaces after annealing to 900 K are attributed to deposited boron adatoms.

The fluorine 1s XPS region is shown in Figure 6.7 for the nearly-stoichiometric surface (top) and the oxygen-terminated surface (bottom). For the nearly-stoichiometric and oxygen-terminated surfaces, one F 1s feature appears at a binding energy of 686.5 eV with the exposure of 5L of $BF_3$. Fluorine in the acid/base adduct $NH_3$:$BF_3$ has a reported F 1s binding energy of 686.6 eV [8]. Because of the similarity in the fluorine binding energy, the F 1s feature at 686.5 eV is attributed to molecular $BF_3$ at base sites. A XPS spectrum taken after heating to 340 K to remove molecular $BF_3$ from the nearly-stoichiometric surface shows a shift to a lower binding energy of 685.9 eV for the F 1s feature. This feature falls in the range of a variety of metal-fluorine compounds (i.e., $MnF_2$ and $CuF_2$) [8]. Therefore, the fluorine from dissociated $BF_3$ remaining on the nearly-stoichiometric surface after 340 K is likely bound at surface metal (i.e., Cr) sites. On the oxygen-terminated surface, the F 1s feature remains around 686.5 eV upon heating to 500 K, removing all molecular $BF_3$ from the surface. This F 1s feature does not shift down in binding energy due to the unavailability of Cr sites to the surface [5]. Hence, the surface fluorine from $BF_3$ dissociation that remains must be bound as F adatoms or $BF_x$ fragments on the oxygen-terminated surface.

The amount of residual boron left on the surface after a 5 L $BF_3$ exposure at 125 K gives a coverage that is similar to the saturation coverage obtained by repeated $BF_3$ exposures in TDS. The extent of boron uptake during TDS experiments can be estimated from the XPS data using a simple model based on the exponential decay of signal with

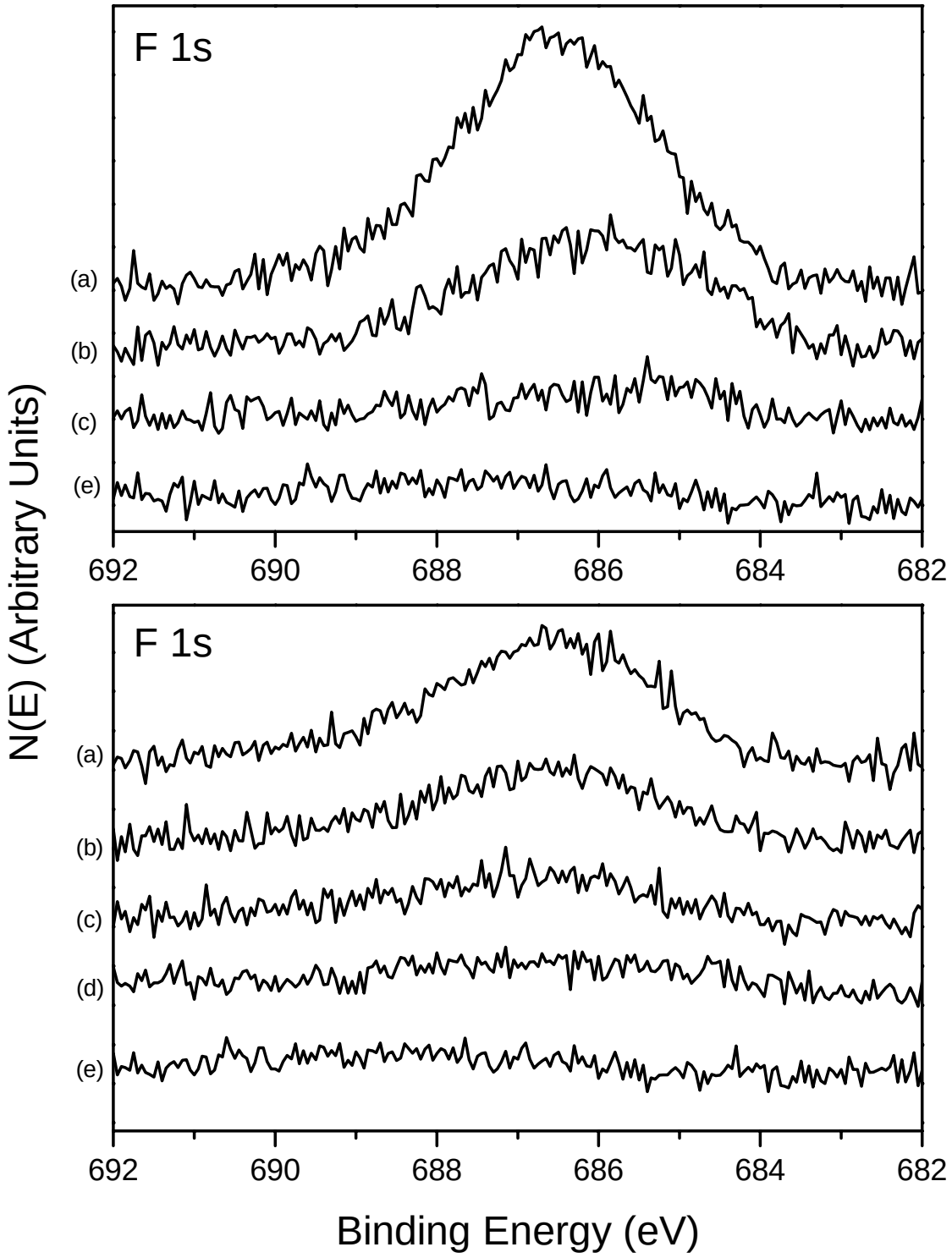


**Figure 6.7 XPS spectra shows the F 1s region of the nearly-stoichiometric $Cr_2O_3$ $(10\bar{1}2)$ surface (top) and the oxygen-terminated $Cr_2O_3$ $(10\bar{1}2)$ surface (bottom) for: (a) a 5 L $BF_3$ exposed surface, (b) a surface annealed to 340 K, (c) a surface annealed to 500 K, (d) a surface annealed to 900 K, and (e) a clean surface.**

sampling depth. Estimates of the expected XPS B/O ratios were made assuming: (1) an exponential decay of signal intensity with distance for normal emission; (2) no diffraction effects; and (3) inelastic mean free paths of 10.0 Å for Cr 2p ($E_{kin}$ = 670 eV) and 10.1 Å for O 1s ($E_{kin}$ = 720 eV) photoelectrons. Mean free paths were estimated from the "universal" curve in Ref. [12]. Using a BO bond length of 1.2 Å, estimates of the expected B/O ratio for one boron atom for every exposed oxygen site yield a value of 0.128 for an ideal, unrelaxed, stoichiometric surface and a value of 0.110 for an ideal, unrelaxed, oxygen-terminated surface [13]. A boron to oxygen XPS ratio determined from peak areas for a 5 L $BF_3$ exposed surface yields a value of 0.078 for the nearly-stoichiometric surface and 0.058 for the oxygen-terminated surface [9]. Therefore, the estimated coverage following a 5 L $BF_3$ exposure is estimated to be approximately 0.6 boron molecules per surface oxygen anion for a nearly-stoichiometric surface and 0.5 boron molecules per oxygen site (terminal chromyl oxygen or three-coordinate oxygen anion) for an oxygen-terminated surface. A boron to oxygen XPS ratio of 0.035 is found for the nearly-stoichiometric surface after annealing to 340 K, removing molecular $BF_3$ from the surface. Hence, the remaining residual boron has an estimated coverage of 0.27 boron molecules per oxygen anion on the nearly-stoichiometric surface. A boron to oxygen XPS ratio of 0.024 is found after annealing to 500 K, removing all molecular $BF_3$ from the oxygen-terminated surface. Hence, the remaining residual boron has an estimated coverage of 0.22 boron molecules per oxygen site on the oxygen-terminated surface.

## 6.4 Discussion

$BF_3$ is not a traditional acidic probe molecule for studying surface basicity. The O 1s XPS results in Figure 6.5 indicate that $BF_3$ forms an adduct with basic surface oxygen anions on $Cr_2O_3$ $(10\bar{1}2)$. The donation of electrons from oxygen to $BF_3$ is accompanied by an increase in the binding energy of the oxygen 1s signal in XPS [11].

$BF_3$ clearly probes differences in coordination of oxide ions on $Cr_2O_3$ $(10\bar{1}2)$. On the nearly-stoichiometric surface where only three-coordinate $O^{2-}$ anions are exposed, TDS of $BF_3$ (shown in Figure 6.1) shows only one desorption feature representative of $BF_3$ desorption from these sites. When the Cr cations are terminated with chromyl oxygens, TDS of $BF_3$ (shown in Figure 6.1) gives an additional high temperature desorption feature representative of $BF_3$ desorption from the terminal oxygen species. The two types of oxygen sites are clearly distinguished in TDS because of their widely different desorption temperatures.

The heats of adsorption of an acidic probe molecule can be interpreted as a measure of the strength of the Lewis acid/base interaction [14]. For cases of unactivated adsorption, the activation energy of desorption measured in XPS should be indicative of the heat of adsorption. The heat of adsorption of $BF_3$ on the terminal chromyl oxygens, 31.8 kcal/mol, is larger than the heat of adsorption on three-coordinate $O^{2-}$ anions, 21.3 kcal/mol. Therefore, the $BF_3$ surface interactions indicate that terminal chromyl oxygens on the oxygen-terminated surface are stronger base sites than three-coordinate $O^{2-}$ anions on the nearly-stoichiometric surface. For $V_2O_5$ (010), Yin *et.al*. found that terminal vanadyl oxygens act as the most favorable adsorption sites among the three types of surface oxygens for the hydrogen bonding of molecular $H_2O$ [15]. In their study of

dissociation of $H_2O$ using periodic first-principles density functional calculations, the adsorption abilities of the surface oxygens correlate with their electron-donating ability [15]. The vanadyl oxygens on $V_2O_5$ are very similar to the chromyl oxygens on $Cr_2O_3$, which are probed by $BF_3$ in TDS as having the highest $BF_3$ heat of adsorption (i.e., strongest electron-donating ability) of any surface oxygens on $Cr_2O_3$.

Although the heats of adsorption of molecular $BF_3$ measured in TDS demonstrate that terminal oxygen on $Cr_2O_3$ is a stronger Lewis base than three-coordinate surface oxygen anions, the O 1s XPS results for the higher binding energy features seen upon $BF_3$ adsorption show the opposite trend one would expect. A higher binding energy is seen for the adsorbed $BF_3$ O 1s feature in XPS on the nearly-stoichiometric surface compared to the oxygen-terminated surface suggesting a greater degree of charge transfer to the adsorbed $BF_3$ from the surface three-coordinate $O^{2-}$ anions than the terminal chromyl oxygens. However, that the O 1s XPS results are believed to be an indication of differences in the electronic properties of the surface oxygen atoms associated with the two adsorption sites, and not a simple measure of the extent of charge transfer from the oxygen atom to the adsorbed Lewis acid. One potential explanation for the apparent discrepancy between the O 1s binding energies and the heat of adsorption at the different binding sites could involve differences in the extent of charge transfer from Cr to O following $BF_3$ adsorption. The Cr=O bond associated with the terminal oxygen should be significantly more covalent than the Cr-O bonds associated with the three-coordinate surface lattice oxygen. Charge transfer from the Cr to the terminal oxygen following $BF_3$ adsorption could account for a lower net charge transfer from the terminal oxygen that would show up as a smaller binding energy shift for the O 1s XPS feature. The

differences in B 1s binding energies observed following $BF_3$ adsorption on the stoichiometric and oxygen terminated surfaces lend some support to this view. There is evidence from gas-phase photoemission studies that the B 1s binding energy in $BF_3$ acid/base adducts tracks the extent of charge transfer to B from the associated Lewis base [16]. Although the B 1s XPS features observed immediately following a $BF_3$ dose cannot be unambiguously attributed to a single type of molecularly adsorbed species, the 0.3 eV lower binding energy observed initially for the oxygen-terminated surface suggests greater charge transfer to boron for adsorbed $BF_3$ at terminal oxygen sites than from three-coordinate oxygen anion sites on the stoichiometric surface. A computational investigation of this adsorption system would be useful as it could shed light on the relative importance of steric and electronic effects in determining the heat of adsorption at the two different types of surface oxygen sites.

The use of $BF_3$ as a probe molecule is complicated by some dissociation and build-up of boron and fluorine on the surface after a $BF_3$ exposure. $BF_3$ dissociates on $Cr_2O_3$ and forms HF and $F_2$ as products. The hydrogen in the HF product probably originates from dissociation of water from the background. Some fluorine and boron adatoms from dissociated $BF_3$ remain on $Cr_2O_3$ $(10\bar{1}2)$ surfaces after annealing to 900 K. On $Cr_2O_3$ $(10\bar{1}2)$ surfaces, many halogenated compounds have dissociated into halogen fragments left at chromium sites [17]. Therefore, the residual fluorine from dissociated $BF_3$ stays at chromium sites if available on $Cr_2O_3$, while the residual boron from dissociated $BF_3$ remains as boron adatoms or $BF_x$ fragments on the surface after annealing to 900 K.

In TDS, $BF_3$ desorption features shift to lower temperatures with increasing $BF_3$ exposures for both the nearly-stoichiometric and oxygen-terminated surfaces. Molecular $BF_3$ in Lewis adducts is expected to change from a planar molecular geometry to a tetrahedral geometry when bound to a Lewis base [4]. Hence, the $BF_3$ adsorbates are expected to acquire a dipole moment upon interaction with basic surface sites. Repulsive interactions between the dipoles of $BF_3$ in the adlayer are the likely cause of the $BF_3$ desorption features shifting to lower temperatures with increasing coverage.

To our knowledge, $BF_3$ has not been used previously as a probe of surface basicity. Conversely, $CO_2$ is one of the most common probe molecules used in measuring basicity [18]. $BF_3$ and $CO_2$ interact very differently on $Cr_2O_3$ $(10\bar{1}2)$ surfaces. The heats of adsorption of $BF_3$ and $CO_2$ show opposite trends between the nearly-stoichiometric and oxygen-terminated surfaces [19]. The heats of adsorption of $BF_3$ on $Cr_2O_3$ indicate that terminal chromyl oxygens on the oxygen-terminated surface are stronger Lewis base sites than the three-coordinate $O^{2-}$ anions on the nearly-stoichiometric surface, while the heats of adsorption of $CO_2$ are larger on the nearly-stoichiometric surface [19]. These differences are primarily due to variations in the adsorbate geometry of $CO_2$ with surface condition. $BF_3$ interacts directly with the oxygen anions on both $Cr_2O_3$ surfaces, but the interaction of $CO_2$ is not as straightforward. $CO_2$ forms a bidentate carbonate on the nearly-stoichiometric surface, which requires an interaction with cation/anion site pairs [19]. On the oxygen-terminated surface, a monodentate adsorbate is formed with the predominant interaction between terminal oxygen and $CO_2$ [19]. Because of differences in the coordination geometry, $CO_2$ does not probe the same types of surface sites on the two surfaces. Since the

bidentate carbonate involves the adsorption of $CO_2$ at a cation/anion site pair, it is clear that $CO_2$ is not a simple probe of surface oxide ions.

## 6.5 Conclusions

$BF_3$, while not a standard probe molecule, has been tested as a probe of the surface basicity of oxygen anions on $Cr_2O_3$ $(10\bar{1}2)$ surfaces. $BF_3$ clearly probes differences in three-coordinate $O^{2-}$ anions and terminal chromyl oxygen (Cr=O) on $Cr_2O_3$ $(10\bar{1}2)$. Heats of $BF_3$ adsorption show that terminal chromyl oxide anions are stronger Lewis bases than three-coordinate $O^{2-}$ anions. $BF_3$ adsorbates interact directly with surface oxygen making it a direct probe of oxygen "base" sites on $Cr_2O_3$. The use of $BF_3$ as a probe molecule is complicated by some dissociation and the slow build-up of surface boron and fluoride during consecutive thermal desorption runs, although the heat of adsorption is not changed significantly with the deposition of boron and fluoride. Heats of adsorption of $BF_3$ show an opposite trend for characterizing the apparent basicity of $Cr_2O_3$ surfaces than the heats of adsorption of $CO_2$.

## 6.6 References


[1] M.A. Barteau, *J. Vac. Sci. Technol. A*, **11** (1993) 2162.
[2] P.C. Stair, *J. Am. Chem. Soc.*, **104** (1982) 4044.
[3] F.A. Cotton, G. Wilkinson, C.A. Murillo, and M. Bochmann, **Advanced Inorganic Chemistry**, Wiley & Sons, New York, 1999.
[4] H.S. Booth, **Boron Trifluoride and Its Derivatives**, Wiley & Sons, New York, 1949.
[5] Steven C. York, Mark W. Abee, and David F. Cox, *Surface Science*, **437** (1999) 386.
[6] C.D. Wagner, W.M. Riggs, L.E. Davis, J.F. Moulder, and G.E. Muilenberg, **Handbook of X-Ray Photoelectron Spectroscopy**, Perkin-Elmer, Eden Prairie, MN, 1979.
[7] J.S. Foord and R.M. Lambert, *Surf. Sci*., **169** (1986) 327.
[8] J.F. Moulder, W.F. Stickle, P.E. Sobol, K.D. Bomben, and J. Chastain, **Handbook of X-Ray Photoelectron Spectroscopy**, Perkin-Elmer, Eden Prairie, MN, 1992.
[9] The Leybold sensitivity factor for B 1s is 0.101.
[10] P.A. Redhead, *Vacuum*, **12** (1962) 203.
[11] G.A. Somorjai, **Introduction to Surface Chemistry and Catalysis**, Wiley & Sons, New York, 1994.
[12] W.M. Riggs, M.J. Parker, in: A.W. Czanderna (Ed.), Methods of Surface Analysis, Elsevier, Amsterdam, 1975, p. 103.
[13] R.C. Weast (Ed.), Handbook of Chemistry and Physics, The Chemical Rubber Co., Cleveland, OH, 1971.
[14] K. Tanabe, M. Morrison, Y. Ono, and H. Hattori, **New Solid Acids and Bases,** Elsevier, New York, 1989.
[15] X. Yin, A. Fahmi, H. Han, A. Endou, S.S.C. Ammal, M. Kubo, K. Teraishi, and A. Miyamoto, *J. Phys. Chem. B*, **103** (1999) 3218.
[16] M. Barber, J.A. Connor, M.F. Guest, I.H. Hillier, M. Schwarz, and M. Stacey, *J. Chem. Soc. Faraday Trans. 2*, **69** (1973) 551.
[17] S.C. York and D.F. Cox, unpublished data.
[18] K. Tanabe, **Solid Acids and Bases**, Academic Press, New York, 1970.
[19] M.W. Abee, S.C. York, and D.F. Cox, *J. Phys. Chem. B*, **105** (2001) 7755.